Cement & Concrete Composites 31 (2009) 358–368

Contents lists available at ScienceDirect

Cement & Concrete Composites

journal homepage: www.elsevier.com/locate/cemconcomp

Performance of cementitious building renders incorporating natural and industrial pozzolans under aggressive airborne marine salts

Khandaker M.A. Hossain [a,*], Mohamed Lachemi [a], Mustafa Şahmaran [b]

[a] Department of Civil Engineering, Ryerson University, 350 Victoria St., Toronto, ON, Canada
[b] Department of Civil Engineering, Gaziantep University, 27310 Gaziantep, Turkey

ARTICLE INFO

Article history:
Received 20 December 2008
Received in revised form 23 March 2009
Accepted 28 March 2009
Available online 7 April 2009

Keywords:
Sea spray
Marine salts
Mortars
External renders
Salt penetration resistance
Fly ash
Volcanic ash

ABSTRACT

This paper presents the results of a study that evaluated the accumulation of marine salts in the metropolitan area of the port city of Chittagong in Bangladesh, and their effects on specimens made from five different types of mortars normally used as external renders for built infrastructures such as buildings and bridges. Mortar specimens were exposed to atmospheric environment at 12 monitoring stations scattered around Chittagong's metropolitan area. Mortars were made (using combinations of cement, lime, volcanic ash, and fly ash) with variable water-to-binder ratios and cement/binder content. The performance of the mortar specimens was evaluated based on marine salt accumulation and resistance to marine salt penetration. The amount of salts (Cl^- and SO_4^- captured in powdered samples extracted from mortar specimens was determined using ion chromatography. Laboratory tests such as mercury intrusion porosimerty (MIP), differential scanning calorimetry (DSC), accelerated chloride ion diffusion (ACID), and electrical resistivity (ER) were conducted on mortars, in addition to tests on fresh and hardened properties of mortars. Test results showed that the marine salt accumulation was significant up to a distance of about 200 m from the seashore. The analysis of accumulation and subsequent penetration of marine salts in exposed specimens identified the mortar types that are more resistant to the aggressive potential of the region's marine aerosol. The results suggest that volcanic ash and fly ash based mortars can provide better salt penetration resistance than cement based mortars. Recommendations of this study will be useful for local authorities engaged in selecting protective measures (in terms of external renderings) to improve the durability of infrastructures exposed to marine salts.

1. Introduction

Sea spray, composed primarily of seawater and particles naturally generated by wind on the seawater surface, introduces ionic species into the atmosphere, principally chlorides and sulfates [1,2]. Air containing sea spray (marine aerosol) causes the accumulative deposition of ions on the external surfaces of structures, which then penetrate the interior of the material through ionic diffusion, causing degeneration. Such environments are extremely dangerous to construction materials; salts can penetrate and crystallize inside the material, causing deterioration of the physical infrastructure, affecting durability, and reducing service life [3–6].

Deterioration of the built infrastructure due to marine salts in coastal regions has been a significant and ongoing problem. This type of infrastructure degradation is primarily true for mortars where salt crystallization inside the mortar pores causes an increase in volume, resulting in high-pressure build-up and subsequent destruction of the pore structure of the material [6]. Most building materials of mineral origin (commonly used as external renders) cannot resist this pressure. Besides salt crystallization within the pores of the external renders, chemical attacks due to the combined action of the penetration of humidity and the sulfates can also occur. Researches have been conducted on the production/distribution of salts from marine aerosols and on the interaction with structures that causes deterioration [3,5–19].

Marine aerosols may be generated by the ocean or by the surf, through bursting bubbles generated by ocean whitecaps, particles torn from crests of ocean whitecaps or breakers on the shore [12,18]. Production of salt in the ocean adjacent to the coast depends on whitecap activity and general ocean wind [18]. The mechanism of deposition of atmospheric components involves transportation of material through the air by advection and diffusion processes and is especially affected by meteorological variables. Besides advective flux, turbulent flux can also play an important role in the transportation and deposition of marine aerosol [16]. Meteorological factors such as wind velocity, wind direction, relative air humidity, rainfall, cloud height, and air temperature can contribute to an increase in particle fall velocity by increasing its mass and density [8,12,18]. The higher the wind

* Corresponding author. Tel.: +1 416 979 5000x7867; fax: +1 416 979 5122.
E-mail address: ahossain@ryerson.ca (K.M.A. Hossain).

0958-9465/$ - see front matter © 2009 Elsevier Ltd. All rights reserved.
doi:10.1016/j.cemconcomp.2009.03.005

velocity, the richer the marine atmosphere is with salts – a condition that favors the generation and emission of sea spray into the atmosphere. Besides meteorological factors, other factors such as surface roughness due to forests and urban landscapes can cause a dramatic fall-off of salt concentration in the air [13,18,19]. It remains a strong tendency for sea salt concentrations to decrease inland and this fact is confirmed from research studies in many countries [7,8,10,14,16,18]. The wet candle device has been used to directly measure the distribution of marine salts in many countries by capturing atmospheric salts on a prescribed area of the apparatus exposed for a particular duration [7,8,18]. Attempt has also been made to correlate salt deposition on the wet candle and those accumulated into concrete [8,19]. However, very few research studies have been conducted on the interaction of salts from marine aerosol with real structures built inland and subsequent mechanism of infrastructure deterioration [7,8,10,11,20].

Bangladesh is a country with a large coastal area that includes the Bay of Bengal. A number of major cities are situated on that coastline, and as a result, materials and products used in construction are negatively affected by the action of airborne marine salts due to sea spray. Chittagong, the nation's second-largest city, is the chief sea port and main centre of export/import in Bangladesh. Over the past decade, the city has rapidly expanded with the establishment of heavy, medium, and light industries, with a resulting rapid population growth. The intense presence of sea spray – a strong marine aerosol with high levels of salt ions – along the city's coastal line and within its greater metropolitan area, creates an adverse environment that has caused tremendous damage to local structures such as buildings and bridges [20]. The presence of strong prevailing wind from sea to land, higher ocean whitecaps and hilly landscape of the region is mainly contributed to the intense presence of sea spray. To date, very little research has been conducted to evaluate the destructive effect of marine aerosol on local infrastructure in Bangladesh.

The purpose of this research is to indirectly evaluate the distribution of marine salts within the greater Chittagong metropolitan region (based on their accumulation on exposed mortar specimens) and to study the effect of marine salts on various mortar mixtures normally used as protective cover for built infrastructures. The performance (in terms of chloride and sulfate penetration resistance) of volcanic ash (VA) and fly ash (FA) based mortars in addition to a locally used mortar is a special feature of the study. The use of industrial wastes (such as FA) and other natural materials (such as VA) offers many advantages from the standpoint of energy/materials conservation, durability enhancement, cost efficiency, lowering greenhouse gas emissions and overall sustainable construction [21–24]. Evaluating the quantity of airborne salts as well as performance of various types of mortars can provide important data for the selection, design, and maintenance of seashore infrastructures in Bangladesh and in various parts of the world, including volcanic areas.

2. Experimental investigations

The study investigated the performance of specimens made from five different types of mortars subjected to marine salt accumulation and subsequent penetration. Twelve monitoring stations were established at different locations of Chittagong metropolitan area (up to 7 km from the seashore) where mortar specimens were kept. The accumulation and penetration of marine salts in exposed mortar specimens kept at these stations were determined over a period of 6 months (26 weeks).

2.1. Mortar mix proportions and material properties

ASTM C270 [25] classifies cement–lime mortar types as M, S, N, and O, depending on the strength needed for an application. Type M mortar has the highest compressive strength, while Type O has the lowest. The mix proportions of the five mortar mixtures (differentiated by cement, lime, VA, FA, sand, and water content) used in this investigation are presented in Table 1.

The cement–lime mortar (falling into the category of Type N in accordance with ASTM C270) commonly used in Bangladesh for external renders was used as control for making specimens to simulate the accumulation of atmospheric aerosol on buildings. Two mortars classified as "N-VA" and "N-FA", made from control N-mortar with the same mix proportions but using 20% VA and 20% FA (as replacement for cement) by weight, respectively. A fourth mortar (named "Local") without lime/VA/FA (weaker than ASTM Type O normally used in rural low-cost construction), was used as a basis for the manufacture of the fifth mortar (named "Local-VA") where 30% of the cement was replaced by VA (Table 1).

Type I Portland cement conforming to ASTM C150 [26], and a fly ash that meets ASTM C618 [27] Class-F requirements were used.

Table 1
Mix composition and characteristics of the used mortar types.

Binder (B) = C + L + VA + FA	Mortar types				
	N (as per ASTM C 270)	N-VA	N-FA	Local	Local-VA
Mix proportions and properties					
Mortar mix proportions					
Cement (C), kg	1.0	0.8	0.8	1.0	0.7
Lime (L), kg	0.7	0.7	0.7	0.0	0.0
Volcanic ash (VA), kg	0.0	0.2	0.0	0.0	0.3
Fly ash (FA), kg	0.0	0.0	0.2	0.0	0.0
Sand (S), kg	5.6	5.6	5.6	12.0	12.0
Water (W), kg	1.4	1.4	1.4	4.0	4.0
Binder (B), kg/m^3	397	403	403	112	113
Cement, kg/m^3	234	190	190	112	79
B/S	0.300	0.300	0.300	0.083	0.083
W/B	0.82	0.82	0.82	4.00	4.00
Mortar properties (fresh and hardened)					
Mass density, kg/m^3	2015	2014	2010	2035	2031
Consistency level, mm	254	256	250	255	258
Water retention, %	95.1	94.5	95.0	96.0	94.0
Air content, %	1.9	1.9	1.9	2.5	2.7
28 days compressive strength, MPa	7.8	7.4	7.5	1.5	1.2
28 days tensile strength, MPa	1.24	1.18	1.20	0.16	0.13
Water absorption after immersion, %	17.2	17.2	17.1	20.0	21.0

Volcanic ash was collected from the Rabaul area of the East New Britain province of Papua New Guinea; the source was a volcano called Mount Tavurvur. A well-graded natural river sand (with a maximum size of 1.2 mm, a fineness modulus of 1.55, a swelling coefficient of 1.38%, specific gravity of 2.61, and water absorption of 1.52%) conforming to ASTM C144 [28] was used. Potable water and a hydrated lime conforming to Type S as per ASTM C207 [29] were also used. Physical and chemical properties of the cement, lime, FA and VA are presented in Table 2.

2.2. Mortar preparation, specimens and testing procedures

The mortars were produced in the laboratory using a mortar-mixer. All sand, hydrated lime, VA, and FA (as required) were first added to 80% of the water and mixed for one minute. Then all the cement and remaining water were added and mixed for another 4 min. The fresh properties of mortars such as consistency, incorporated air content, water retention capacity, and density were determined as per ASTM C185 [30], ASTM C1506 [31], and ASTM C1437 [32], respectively.

Cylindrical (50 mm × 100 mm) mortar specimens were produced. The specimens were removed from the mould after 24 h of casting, and then kept in a chamber at a controlled temperature (23 ± 2 °C) and relative humidity (RH > 90%) until tested or transported to monitoring stations. At the age of 28 days, the cylinder specimens were tested to determine compressive and tensile strengths as per ASTM C39 [33] and ASTM C496 [34], respectively. Water absorption by immersion was also determined at the age of 28 days. The results of these tests are presented in Table 1.

At the age of 28 days and 200 days, an accelerated chloride ion diffusion (ACID) test [35], commonly known as "migration test", was used to determine the chloride ion diffusion coefficient of the mortars. In this test, a diffusion cell (volume: 785 ml) using 3% NaCl and 0.3 N NaOH as cathode and anode solutions, respectively, was used. Mortar specimens of 50 mm diameter and 20 mm thickness were placed between the electrodes and an electric field of 3 V/cm was applied to the electrodes. The amount of chloride ions (Cl^-) that migrated from the cathode through the mortar specimen to the anode of the cell was determined by measuring the concentration of the chloride ions in the anode solution periodically. The amount of chloride ions (Cl^-) vs. time (days) produces a straight line, and the slope of this straight line is termed "chloride ion flux" (f_i). f_i was used in the Nernst–Plank equation (Eq. (1)) to calculate the chloride diffusion coefficient (D_i) [35]:

$$D_i = \frac{RTf_i}{I_c F C_i \delta V} \quad (1)$$

where D_i = chloride ion diffusion coefficient in cm^2/s, R = universal gas constant = 8.314 J/K mol, T = temperature in Kelvin, I_c = ionic charge of chloride ion, F = Faraday constant = 9.65×10^4 C/mol, C_i = chloride ion concentration in the anode chamber of the diffusion cell, and δV = electric field in V/cm.

The electrical resistivity of mortars was measured at the age of 28 days and 200 days with an automatic LCR (inductance 'L', capacitance 'C', resistance 'R') meter by applying a 10 mV AC at 1 kHz across saturated specimens (50 mm diameter × 50 mm thickness) using copper plate electrodes [36]. The instrument gave a digital display of the value of the electrical resistance, which was used to calculate electrical resistivity.

The porosity and pore size distribution in terms of total pore volume (TPV) were measured using mercury intrusion porosimetry (MIP), which had a measuring pressure ranging from 0.01 MPa to 200 MPa [36]. The contact angle selected was 140° and the measurable pore size ranged from 0.004 MPa to 144 μm. The samples, which were in the form of pellets of about 5 mm in size, were collected from the mortar specimens at 28 and 200 days and immediately soaked in acetone to stop further hydration. The samples were dried in an oven at 60 °C for 48 h before testing.

After 28 days, the cylinder specimens were also transported to the monitoring stations to study the accumulation and subsequent penetration of marine salts from the atmospheric aerosol over a period of 6 months.

2.3. Monitoring network and exposure conditions for mortar specimens

In order to study the influence of the aggressive potential of atmospheric marine salts on regional constructions, cylindrical specimens manufactured from five types of mortar were exposed to atmospheric marine salts in 12 monitoring stations. A satellite map showing the locations of 12 stations in the greater Chittagong metropolitan area is presented in Fig. 1. The stations were designated and identified by their distance from the coastal line, which varied from 50 m to about 7 km. In order to reduce the effect of ground roughness and ensure the safety of exposed mortar

Table 2
Physical properties and chemical composition of cement, lime, VA, and FA.

	Cement	Lime	Fly ash	Volcanic ash
Physical properties				
Specific gravity	3.14	2.32	2.08	2.15
Blain fineness, cm^2/g	3740	–	3060	2850
Passing a 200 mesh Sieve, %	–	86.2	–	–
Chemical composition (%)				
Silicon dioxide (SiO_2)	19.4	0.61	52.4	59.3
Aluminium oxide (Al_2O_3)	5.3	0.26	23.4	17.5
Ferric oxide (Fe_2O_3)	2.3	0.18	4.7	7.0
Calcium oxide (CaO)	61.8	41.6	13.4	6.1
Magnesium oxide (MgO)	2.3	29.5	1.3	2.6
Sodium oxide (Na_2O)	0.2	0.08	3.6	3.8
Potassium oxide (K_2O)	1.1	0.04	0.6	2.0
Equivalent alkali ($Na_2O + 0.658K_2O$)	0.9	0.11	4.0	5.1
Sulphur trioxide (SO_3)	3.8	0.14	0.2	0.7
Loss on ignition	2.1	27.2	0.3	1.03
Bogue potential compound composition (%)				
Tricalcium silicate (C_3S)	53.8	–	–	–
Dicalcium silicate (C_2S)	15.2	–	–	–
Tricalcium aluminate (C_3A)	10.2	–	–	–
Tetra calcium aluminoferrite (C_4AF)	7.1	–	–	–

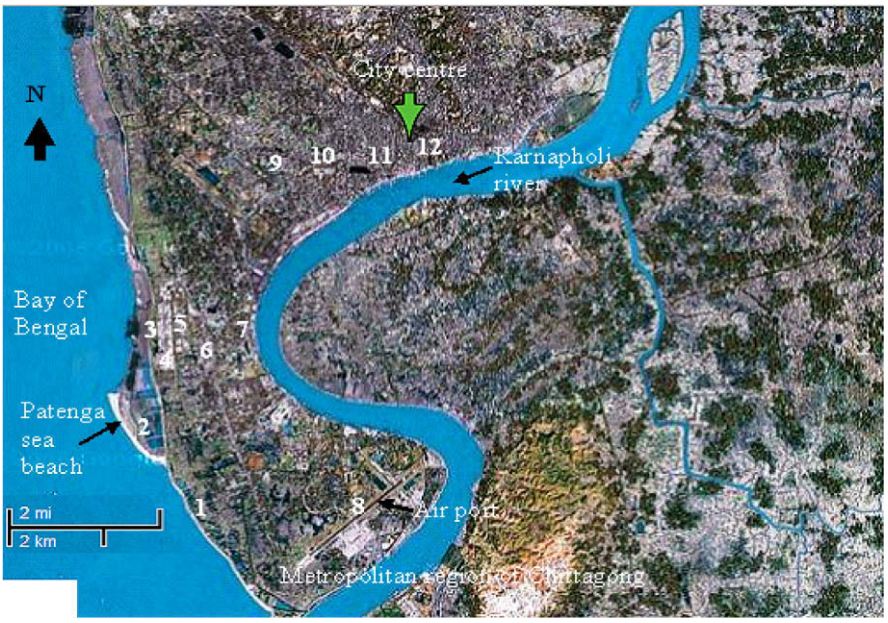

Fig. 1. Satellite map of the metropolitan region of Chittagong showing sampling stations.

specimens, the stations were selected based on the availability of an open area with cover and good wind circulation, and no interference from walls, trees, or other elements.

Mortar test specimens were placed at each of the stations for exposure to atmospheric aerosol for a duration of 6 months (25 weeks from April to September 2000) in order to identify the effects of marine salts on the external renders (classified by five types of mortars) (Fig. 2). The positioning of the set of test specimens stayed constant in relation to the prevailing direction of the local wind. The exposure duration of 6 months is critical and justifiable because the prevailing wind from the south (sea) to the south-east (land) and the higher wind speed bring more sea aerosol to the land from the sea. As the study was concentrated on the cumulative accumulation of marine salts at the sampling stations during the whole study duration, it did not address the effect of varying meteorological conditions or the correlation between the accumulation of marine salts and the meteorological parameters, or parameters associated with ocean's aerosol production.

2.4. Analysis of marine salts using ion-chromatography

To determine the salt content accumulated in various cylindrical mortar specimens, samples were removed from two diametrically opposite points (0.5 cm from the external surface) named "outer" and from the centre point, name "centre" (Fig. 2). This

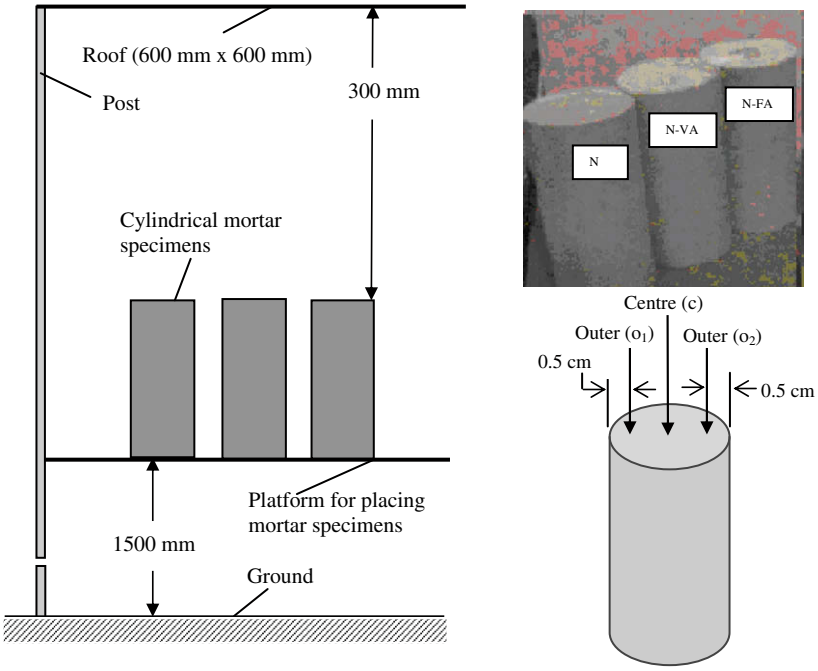

Fig. 2. Typical exposed mortar specimens at a sampling station.

allowed the determination of the penetration of the salt ions deposited on the surface (from atmospheric aerosol) to the inside of the specimens. Material was removed for analysis using an electric drill. At each of the points, a 4 cm diameter hole was drilled to collect an average of 3 g of powder for analysis; the powder was stored in small polyethylene flasks. The ions were then extracted in deionized water at ambient temperature by means of ultrasound bath for 20 min. The extraction water was then analyzed by the ion-chromatographic (IC) method using QuikChem 8000 [37]. A typical IC system consists of a liquid eluent, a height-pressure pump, a sample injector, an analytical column, and a detector with chemical suppression.

The chloride in mortar/concrete can be considered to be chemically bound (incorporated in solids), physically bound (adsorbed), or free in aqueous pore solution [38]. Extraction of concrete with nitric acid (as is the case for potentiometric titration procedure) yields total chloride (both free and bound). Extraction with water generally yields the free chloride, as is the case for IC. One of the problems associated with extraction of chloride from mortar by either water or acid is variable efficiency. IC used for the determination of chloride in mortar – and in the chloride migration study – yielded better precision [38]. In this study, the choice of using IC (besides its precision) was based on the premise that only free chloride is significant in the corrosion process and hence, it is important to study the comparative performance of different types of mortars as building renders against salt penetration. Chemical reactions occur inside building overlay materials, producing insoluble salts that cause part of the damage encountered in mortars, as in the case of sulfatation processes. In this study, only the deposition/formation of soluble salts of the ions is considered aggressive to the overlay material. The method of analysis of salts (both chloride and sulfate ions) by IC provided results that were equivalent to that of ISO method 10304 [39].

The actual concentrations of chloride (Cl^-) and sulfate (SO_4^-) ions derived from the atmosphere in the specimens after exposure were obtained by deducting the concentration of these ions in the blanks (respective mortar specimens kept in the laboratory and not exposed to the atmospheric aerosol) from the concentration of salts in the exposed mortar specimens.

2.5. Analysis of mortar samples by differential scanning calorimetry (DSC)

The differential scanning calorimetry (DSC) test was also performed on mortar samples taken from the specimens exposed to marine salts for the duration of 6 months to quantify the formation of Friedel's salt ($C_3A{\cdot}CaCl_2{\cdot}10H_2O$) and $Ca(OH)_2$. The mortar samples used weighed around 60 mg. The samples were heated at a constant heating rate of 10 °C/min to 1100–1200 °C, in a dynamic helium atmosphere. The DSC data analysis gave graphs of heat flow between the sample and reference crucibles vs. temperature. DSC thermograms showed peaks due to endothermic (heat absorbing) and exothermic (heat releasing) reactions. The $Ca(OH)_2$ and Friedel's salt contents are equivalent to the area (enthalpy) under the respective endothermic peaks. The presence of $Ca(OH)_2$ and Friedel's salts as an endothermic peak was observed at around 450 °C and 300 °C, respectively.

3. Results and discussion

3.1. Climatic characteristics of the region

Bangladesh is situated between 20°34′–26°38′ North Latitude and 88°01′–92°41′ East Longitude. The country has a 724-km long coast line and many small islands in the Bay of Bengal. Since the country is situated close to the equator, aerosol production in the Bay of Bengal is expected to be lower than high or low altitudes such as Australia and Europe. The weather in Bangladesh is largely governed by the monsoon. In Chittagong, wind blows from the north-east (from land to sea) in the winter season and from the south-east (sea to land) during the summer season. The wind speeds exhibit strong seasonal cycles, and are lower in the September–February period and higher in the March–August period. The wind also exhibits a diurnal cycle; it generally peaks in the afternoon and is weakest at night. Frequency greater than 4 m/sec was above 70% in June, compared with less than 7% in November. During the duration of this study (April–September), wind speed ranged from 2.9 m/s to 5.8 m/s (with a mean of 4.6 m/s), temperature ranged from 27 °C to 32 °C, humidity ranged from 78% to 88%, and total rain fall was around 210 cm. The meteorological parameters such as temperature, humidity and rain fall did not considerably vary during the duration of study. The wind speed also did not vary significantly between May and September.

3.2. Mortar properties

The fresh properties of mortars such as consistency, incorporated air content, water retention capacity, and mass density are presented in Table 1, along with the 28-day compressive and tensile strengths and water absorption properties. Table 3 presents the results of ACID, ER, MIP, and DSC test results. As seen from Table 1, the addition of VA/FA slightly reduced the 28-day strength of mortars, although strength is expected to improve in the long-term due to pozzolanic action of VA/FA [23,24].

Table 3 shows that the diffusion coefficient (D_i) (from ACID test) decreases with the increase of curing time (from 28 days to 200 days) for all mortars and the addition of FA or VA in mortars (N-VA, N-FA, and Local-VA) produces lower D_i values. Lower D_i values can be attributed to the beneficial effect of VA/FA in increasing the long-term chloride penetration resistance of VA/FA based mortars due to the continuing hydration of cement and VA/FA, which is beneficial in reducing pore sizes and densifying matrix.

The electrical resistivity (ER) of the VA/FA based mortars is higher and also increases rapidly with time (from 28 days to 200 days) compared with control mortars (Table 3). Electrical current through hydrating cement mortar is electrolytic (mainly due

Table 3
Diffusivity, electrical resistivity, pore size, and DSC test results.

Mix ID	Diffusion coefficient (D_i) ($\times 10^{-7}$ cm^2/s)		Electrical resistivity (ER) (Ω cm)		Pore size (<20 nm) (% of TPV)		DSC test results	
							Friedel's salt (J/g)	$Ca(OH)_2$ (J/g)
	28 days	200 days	28 days	200 days	28 days	200 days	200 days	200 days
N	1.5	0.9	12	22	15	20	8	65
N-VA	1.3	0.7	13	32	20	30	12	34
N-FA	1.3	0.7	13	36	20	33	13	36
Local	2.0	1.6	6	9	10	13	5	45
Local-VA	1.9	1.1	8	16	12	20	9	22

to the flow of ions through the pore spaces), hence ER is an indirect measurement of porosity and diffusivity [40]. The high ER of VA/FA based mortars would enhance their overall resistivity against marine salt penetration.

VA and FA are added as fine granulates; upon hydration they have the capability of partially obstructing voids and pores. This leads to a decrease of pore size with refinement of pore structure, and to a smaller effective diffusivity for chloride or other salts, as confirmed from the experimental results of D_i and ER in Table 3. The effect of VA/FA on pore size distribution within the TPV is addressed by presenting pore sizes less than 20 nm (micropores) in mortars at 28 and 200 days (Table 3). The percentage of TPV that is less than 20 nm increases with time and with replacement of cement by VA/FA. This indicates that the addition of VA/FA produces a refinement of mortar pore structure and therefore improved salt penetration/corrosion resistance. Previous studies reported that the addition of fly ash leads to a decrease in concrete porosity, which is directly related to its salt diffusivity [41,42]. A reduction of chloride diffusivity in concrete to half its value was observed as a consequence of a 50% replacement of cement by fly ash [41,42]. Moreover, the chloride binding effect of fly ash reduces the chloride diffusion coefficient.

Table 3 shows the results of DSC for the mortars at a curing age of 28 and 200 days. The quantity of $Ca(OH)_2$ formed in the hydration of the mortar decreases with the addition of VA/FA. Lowering of $Ca(OH)_2$ also indicates that the pozzolanic reactivity of VA/FA consumes $Ca(OH)_2$, resulting from hydration of the cement. The pozzolanic reaction of VA/FA with $Ca(OH)_2$ produces a refinement of pore structure, as observed, and thus improves the salt penetration/corrosion resistance [36]. This is justified from the lower value of D_i, and higher ER in VA/FA based mortars (Table 3).

A portion of the chlorides permeating into the concrete by diffusion along water paths or open pores react with the cement hydration products (mainly tricalciumaluminates – C_3A) to form calcium chloroaluminate hydrate (Friedel's salt) in a process called "chloride binding". Table 3 shows that the quantity of Friedel's salt increases with the addition of VA/FA in the mortar. The presence of higher amounts of reactive alumina in VA/FA may be one of the factors that can adsorb more chloride ions to form Friedel's salts. Higher Friedel's salt formation consequently lowers the levels of free chloride, and hence reduces the chloride ion diffusivity of VA/FA based mortars [43]. On the other hand, "chloride binding" reduces the quantity of C_3A available for the sulfate ions to react and form either gypsum or expansive ettringite, which improves the sulfate resistance of VA/FA based mortars [44]. However, the presence of carbonation can change this situation.

3.3. Accumulation of marine salts in exposed mortar specimens along the sampling network

Tables 4 and 5 present the concentrations of Cl^- and total SO_4^- determined from different types of mortar specimens, after exposure to the atmospheric aerosol for the duration of 25 weeks (6 months). The salt concentration at the outer and central locations of the mortar specimens placed at various stations provided a measure of the variation of salt accumulation with distance from the shore line.

Cl^- accumulation (as per both outer and centre locations) decreased with the increase of the distance from the sea (Fig. 3). Table 4 shows higher Cl^- concentration in test specimens at sampling stations closer to the sea, mainly to about 207 m (sampling station 3). Fig. 4 shows that around 65% of the total Cl^- along the monitoring network was deposited within a distance of 207 m from the shoreline. In other research studies [7,10], about 70% deposition of Cl^- was also observed in the first hundred meters from the sea.

With respect to total SO_4^- the trend of decrease in accumulation with the increase in distance from the sea was not observed (Fig. 5) since a very small portion of this ion (incorporated into the local atmospheric aerosol), had its origin from sea spray. Even at the sites very close to the sea, there was much more enrichment sulfate than chloride in the test specimens (Fig. 3), which indicates that the salts originating from the sea are not the only major source of sulfate in the mortars. The sulfate bearing wastes (diverted into the sea) from the industries near the shoreline can be a factor for higher sulfate accumulation due to sea spray. The exposed mortar specimens were also subjected to the deposition of gases such as SO_2 released from industries and traffic, which also contribute to the accumulation of SO_4^-. Sampling station 8 (at 3.2 km) confirmed this fact, showing lower SO_4^- concentration as it was situated in an area of comparatively lower traffic and no industry. Even though the sea spray is not the main source of the SO_4^-, which is incorporated in the atmospheric aerosol of the region, the performance of

Table 4
Cl^- accumulation in mortar specimens.

Sampling station	Distance from sea (m)	1 (Outer location)					2 (Outer location)					3 (centre location)				
		Mortar type					Mortar type					Mortar type				
		N	N-VA	N-FA	Local	Local-VA	N	N-VA	N-FA	Local	Local-VA	N	N-VA	N-FA	Local	Local-VA
		Cl^- accumulation (μg/g)					Cl^- accumulation (μg/g)					Cl^- accumulation (μg/g)				
1	93	252	237	229	345	328	249	234	228	349	329	170	158	151	292	255
2	152	198	186	180	271	257	190	179	174	266	251	140	130	124	235	210
3	207	145	136	132	199	189	151	142	138	211	199	117	109	104	180	176
4	452	72	68	66	99	94	75	71	69	105	99	53	49	47	88	79
5	811	55	55	57	75	72	57	54	52	80	75	44	41	39	73	66
6	1222	41	39	37	56	53	41	39	38	57	54	30	27	26	49	44
7	2105	33	33	33	45	43	32	30	29	45	42	25	23	22	43	38
8	3216	28	26	25	38	36	26	24	24	36	34	19	18	17	32	29
9	4019	26	24	24	36	34	27	25	25	38	36	19	18	17	28	28
10	5013	21	23	21	29	27	24	23	22	34	32	16	15	14	27	24
11	6105	18	17	16	25	23	18	17	16	25	24	13	12	12	21	19
12	7012	16	16	18	22	21	14	13	13	20	18	11	10	10	18	16
Accumulation (%)[a]		66	65	65	65	66	65	65	65	65	65	65	65	65	65	65
Range of concentration		16–252	16–237	18–229	22–345	21–328	14–249	13–234	13–228	20–349	18–329	11–170	10–158	10–151	18–292	16–255

[a] Accumulation up to 207 m as % of total accumulation along the entire sampling network.

Table 5
SO_4^- accumulation in mortar specimens.

Sampling station	Distance from sea (m)	1 (Outer location)					2 (Outer location)					3 (Centre location)				
		Mortar type					Mortar type					Mortar type				
		N	N-VA	N-FA	Local	Local-VA	N	N-VA	N-FA	Local	Local-VA	N	N-VA	N-FA	Local	Local-VA
		SO_4^- accumulation (μg/g)					SO_4^- accumulation (μg/g)					SO_4^- accumulation (μg/g)				
1	93	2205	2029	1962	2911	2844	2249	2069	2002	2969	2873	1354	1123	1074	2264	2196
2	152	813	748	724	1074	1049	821	756	731	1084	1060	519	431	412	854	828
3	207	730	672	650	964	942	715	658	637	944	951	491	407	390	757	734
4	452	880	810	783	1162	1135	898	826	799	1185	1147	565	468	448	917	881
5	811	859	790	765	1134	1108	851	783	757	1123	1115	579	469	438	939	901
6	1222	895	823	797	1181	1146	877	807	781	1158	1152	563	467	447	914	878
7	2105	886	815	789	1170	1134	904	831	804	1193	1141	597	483	457	993	958
8	3216	507	466	451	669	649	497	457	442	656	653	319	264	253	518	500
9	4019	1003	903	873	1344	1284	993	894	864	1331	1290	632	513	490	960	926
10	5013	1014	912	882	1358	1297	1024	921	891	1372	1304	647	497	485	1067	1046
11	6105	1015	914	883	1360	1299	985	886	857	1319	1306	635	515	493	1047	995
12	7012	980	882	853	1313	1254	960	864	836	1287	1261	616	488	438	1016	966
Accumulation (%)[a]		32	32	32	32	32	32	32	32	32	32	31	32	32	32	32
Range of concentration		507–2205	466–2029	451–1962	669–2911	649–2844	497–2249	457–2069	442–2002	656–2969	653–2873	319–1354	264–1123	253–1074	518–2264	500–2196

[a] Accumulation up to 207 m as % of total accumulation along the entire sampling network.

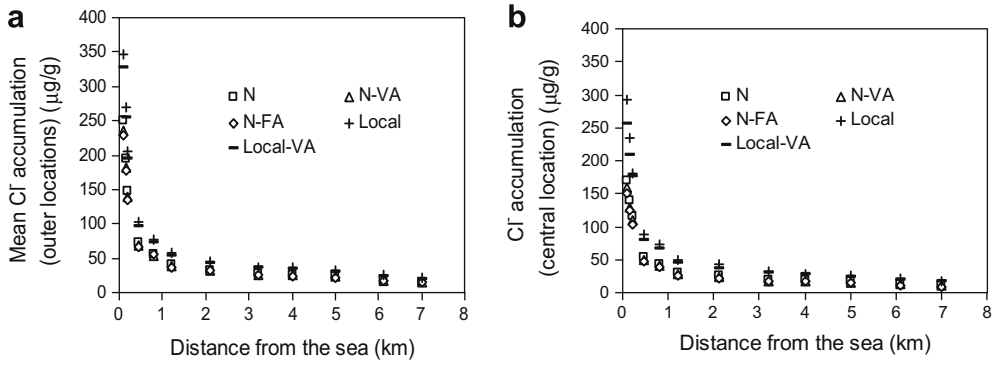

Fig. 3. Mean Cl^- accumulation on mortar specimens: (a) outer and (b) central locations.

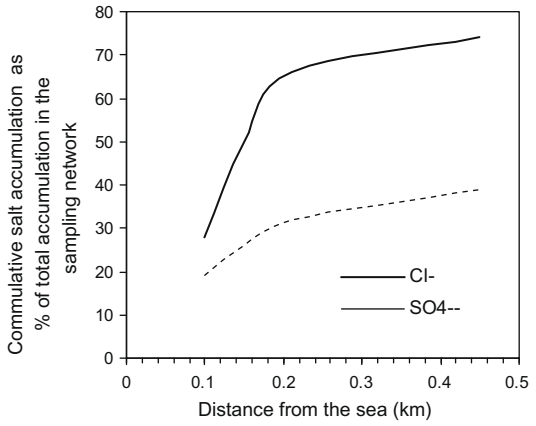

Fig. 4. Cumulative salt accumulation (%) with distance from the sea.

different types of mortars subjected to aggressive SO_4^- is revealed in this study.

Fig. 4 shows that around 32% of the total SO_4^- along the sampling network is accumulated within a distance of 207 m from the shore line. This indicates that the contribution of sea spray to airborne Cl^- deposition is much higher than that of SO_4^- deposition.

Salt deposition, to a certain extent, represents the salt availability in surrounding micro-environments and salt ions are able to accumulate on the surface of the structures (the mortar specimens in this study). It should be noted that the significant amount of salts (present in marine aerosols) did not accumulate on the surface of mortar specimens and thus did not penetrate them. The study also shows that the percentage of available aerosols accumulated depends primarily on turbulence intensity (controlled by upstream ground roughness) and only minimally on aerosol particle size, while total accumulation depends on turbulence intensity, surface area and mean air velocity [19].

3.4. Performance of mortars based on marine salt penetration resistance

The salt accumulation and subsequent penetration into the specimen were found to depend on the type of mortar – they were lowest in Type N and highest in Type "Local" (Figs. 3 and 5). The performance of different mortars in terms of marine salt (Cl^-/SO_4^-) penetration resistance index (SPRI) was studied based on central Cl^-/SO_4^- accumulation expressed as% sum of outer locations presented in Eq. (2):

$$\mathrm{SPRI} = \frac{100 d_c}{d_{O1} + d_{O2}} \tag{2}$$

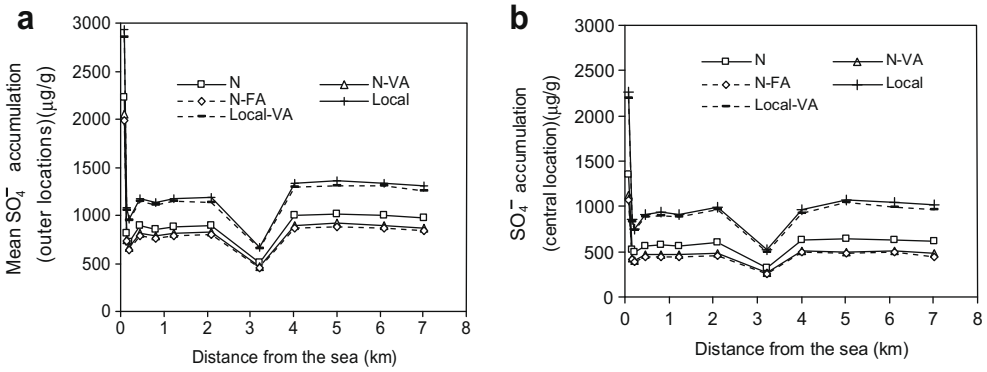

Fig. 5. Mean SO_4^- accumulation on mortar specimens: (a) outer and (b) central locations.

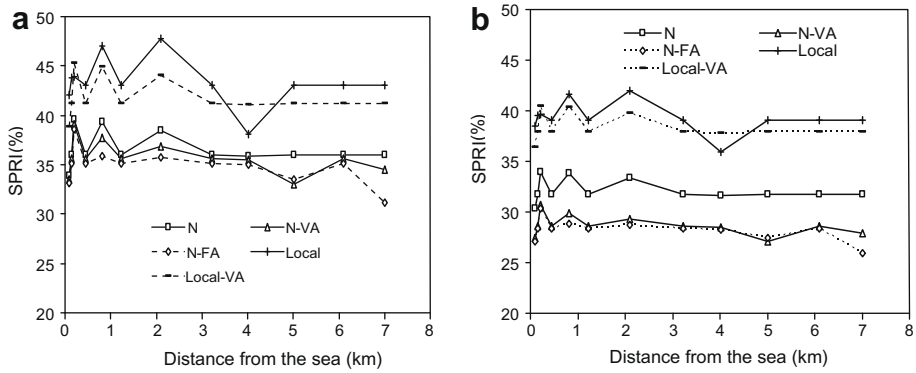

Fig. 6. Performance of mortars based on (a) Cl^- and (b) SO_4^- penetration resistance.

where d_c is the Cl^- or SO_4^- accumulation at the centre location of specimen in μg/g, while d_{O1} and d_{O2} are the Cl^- or SO_4^- accumulation at the outer location 1 and 2, respectively, of the specimen in μg/g (Fig. 2). SPRI provides a measure of penetration of salts from the surface of the specimens to the centre.

Fig. 6 shows the variation of SPRI values for Cl^- and SO_4^- as observed in different types of mortars in sampling stations. It should be noted that a lower value of SPRI indicates higher salt penetration resistance. Figs. 6 and 7 indicate that the Cl^-/SO_4^- penetration resistance is the highest for Type N-FA (mean SPRI of 34.9% for Cl^- and 28% for SO_4^-), followed by Type N-VA (mean SPRI of 35.7% for Cl^- and 29% for SO_4^-), Type N (mean SPRI of 36.6% for Cl^- and 32% for SO_4^-), Type Local-VA (mean SPRI of 41.9% for Cl^- and 38% for SO_4^-), and Local (mean SPRI of 43.4% for Cl^- and 39% for SO_4^-).

It is well known that the much higher diffusion rate of chloride ions (compared with sulfate ions) allows the chloride ions to permeate through the concrete surface much faster than the sulfate ions. Higher SPRI of Cl^- (ranging between 34.9% and 43.4%) compared to SO_4^- (ranging between 28% and 39%) confirmed that the diffusion of Cl^- through the mortar was faster than SO_4^-. It should be noted that capillary sorption also plays an important role in the salt transport in mortar specimens exposed to atmosphere besides diffusion.

Type "Local" mortars (both "Local" and "Local-VA") showed lower resistance to the aggressive action of sea salts with higher values of SPRI compared with all Type "N" mortars (N, N-VA, and N-FA). This result can be attributed to the presence of a low quantity of cement with no lime or binder content as well as higher W/B in "Local" mortars compared with "N" mortars (Figs. 6 and 7). The decrease of cement/binder content in mortars generally increases the porosity/permeability, thereby increasing the penetration and

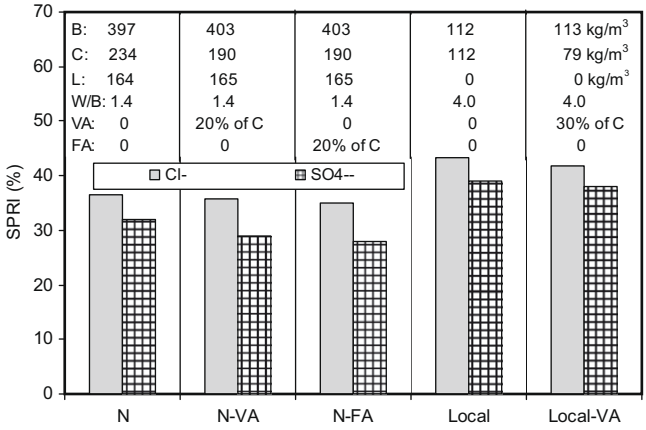

Fig. 7. Comparative salt penetration resistance of mortars in terms of SPRI.

transport of both ions into the material [8]. It was therefore easier for both Cl^- and SO_4^- ions accumulated on the surface of the "Local" mortars to diffuse and migrate to the centre. The higher water absorption capacity of Type "Local" mortars (Table 1) may also render these materials less resistant to the penetration of salt ions via atmospheric water vapor and to the subsequent harmful hydration/crystallization of salts inside.

The addition of VA or FA as replacement of cement in N and "Local" mortars (while keeping binder "B", lime "L", and W/B constant) increases the Cl^-/SO_4^- penetration resistance of mortars (N-VA, N-FA, and Local-VA). This is evident from the lower mean SPRI values of N-VA/N-FA mortars compared with N mortars, as well as

lower SPRI values in Local-VA mortars compared with Local mortars (Figs. 6 and 7). FA mortars showed slightly higher Cl^-/SO_4^- penetration resistance than VA mortars at similar VA/FA content.

3.5. Correlation between laboratory and field salt resistivity characteristics of mortars

Fig. 8 shows a good correlation between D_i and ER based on the combined laboratory experimental data of all mortars at 28 and 200 days, where D_i was found to be inversely proportional to ER. This means that the diffusion coefficient of chloride ion through the mortars could be derived from the value of its electrical resistivity. The relationship between D_i and ER can be expressed as Eq. (3):

$$ER = 654.95(D_i)^{-1.5277} (R^2 = 0.981) \quad (3)$$

where ER is in Ω cm and D_i is in 10^{-8} cm^2/s. Good correlation between D_i and ER obtained in this study is attributed to the measurement of D_i at a steady state condition in ACID test (assume a constant flux of Cl^- from the cathode chamber through the sample into the anode chamber) which does not account for chloride binding. Such correlation is difficult to achieve in the case of non-steady state conditions. However, previous research by Clement et al. [45] showed correlation between ER and D_i in the case of non-steady state condition. Andrade [46] emphasized the importance of establishing a correlation between ER and D_i and described a graphical relationship between them. Since electrical resistivity measurement is simple and nondestructive, development of correlation equations between ER and D_i similar to that developed in this study (Eq. (3)) would be very useful for researchers and for field applications.

Figs. 9 and 10 show that relationships exist between laboratory (D_i and ER) and field (represented as SPRI) diffusivity data of Cl^- and SO_4^- for mortars at 200 days. As expected (for both Cl^- and SO_4^-), a decrease in ER increases SPRI while an increase in D_i increases SPRI. This shows that the SPRI can provide a good measure of marine salt diffusivity in mortars, and that its use to characterize the salt penetration resistance of mortars in this study is justified. ER shows slightly better correlation (compared to D_i) with both Cl^- and SO_4^- SPRI. D_i (based on Cl^- diffusivity) correlates slightly better with Cl^- SPRI than SO_4^- SPRI, which is reasonable. It should be noted that the ACID test method does not necessarily lead to the same migration coefficients as natural diffusion tests, since it is based on constant flux of Cl^- from the cathode chamber through the sample into the anode chamber. Such a constant flux of chloride ions does not exist in practical situations for two reasons: chloride binding/de-binding in cement and the change of OH^- concentration of the pore solution due to the electrochemical reaction

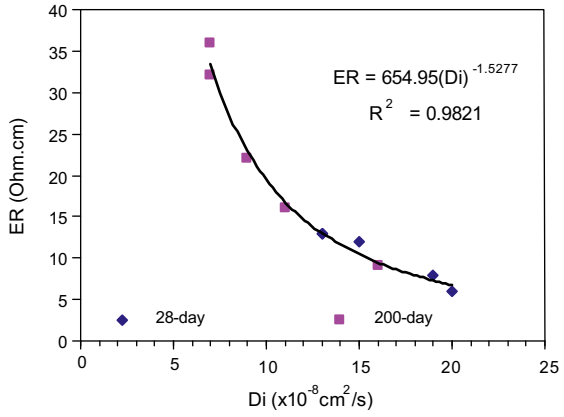

Fig. 8. Correlation between D_i and ER.

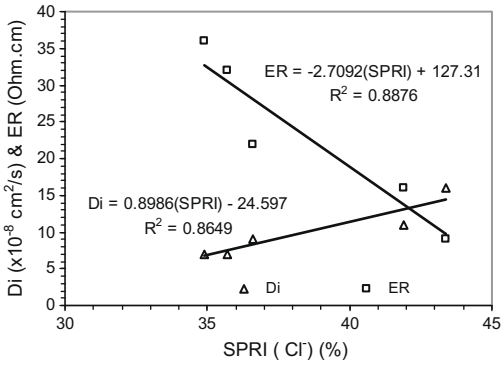

Fig. 9. Correlations between D_i and ER with SPRI (Cl^-) (200 days).

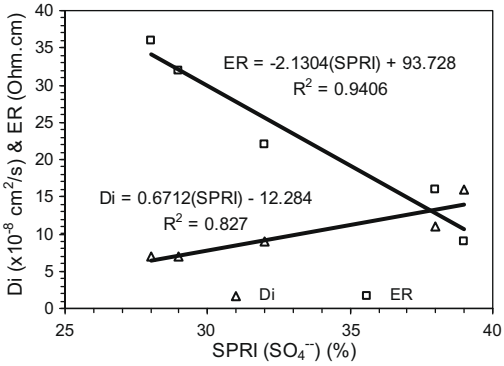

Fig. 10. Correlations between D_i and ER with SPRI (SO_4^- (200 days).

that occurs at the electrodes. This may be attributed to the slightly lower correlation of D_i ($R^2 = 0.86$) compared to ER ($R^2 = 0.89$) with Cl^- SPRI (Figs. 9 and 10).

4. Conclusions

This study has evaluated the hazard potential of marine salt accumulation on the rendering materials (mortars) typically used in construction. The aggressive potential was evaluated by performing comprehensive laboratory tests and studying accumulation/penetration of marine salts in five different types of mortar specimens kept in monitoring stations within the metropolitan area of Chittagong, Bangladesh, at different distances from the sea. The following conclusions are drawn from the study:

- Cl^- accumulation decreased with the increase of the distance from the sea. Based on the accumulation on mortar specimens, around 65% of the total Cl^- along the monitoring network was accumulated within a distance of 207 m from the shoreline. The trend of decrease in accumulation with the increase in distance from the sea was not observed for the case of SO_4^- since a small portion of this ion incorporated into the atmospheric aerosol had its origin from sea spray.
- Generally, mortars with high cement content, lower water absorption capacity, and lower porosity showed strong resistance to penetration of sea salts. As a result, ASTM Type N based mortars showed better salt penetration resistance compared to "Local" mortars having lower cement/binder content.
- The addition of fly ash (FA) or volcanic ash (VA) produced lower chloride ion diffusion coefficient (D_i) of mortars. The electrical resistivity (ER) of VA/FA based mortars was also higher and increased rapidly with age compared with control mortars

(without VA or FA). The higher ER and lower D_i of VA/FA based mortars should enhance the overall resistance of such mortars to marine salt penetration. The higher Cl^- and SO_4^- penetration resistance of VA/FA based mortars was confirmed from the field investigation of mortar specimens subjected to atmospheric marine salt accumulation at the stations along the 7 km-long monitoring network. This beneficial effect of VA/FA is attributed to the refinement of pore structure, and the lowering of the presence of free chloride due to Friedel's salt formation and pozzolanic action, as confirmed in this study.

- Correlations exist between diffusion coefficient (D_i) and electrical resistivity (ER) of mortars. The ER of mortars can be used to predict D_i in order to make the measurement very simple and to make the nature of the test non-destructive.
- Correlations exist between Cl^-/SO_4^- diffusivity of mortars (expressed in terms of salt penetration resistance index "SPRI") exposed to marine salts in field conditions and those obtained in the laboratory from accelerated chlorine ion diffusion (ACID) and electrical resistivity tests (D_i and ER, respectively).
- Choosing a suitable mortar type that can be used as external rendering to concrete structures can minimize the aggressive attack of marine salts and enhance the durability of structures. Low-cost VA/FA based mortars (N-VA, N-FA or Local-VA) with better salt penetration resistance can be used as building renders to protect infrastructures from the aggressive influence of airborne marine aerosol.
- The results of this study should assist in finding and recommending suitable rendering materials for local construction that are compatible with local environmental conditions. They can also help to develop code-based guidelines for the use of such materials in construction and maintenance of built infrastructures. Clearly, the use of the recommended materials can lead to building economical, durable, and sustainable infrastructures with longer service lives.

Acknowledgements

The authors acknowledge the financial and laboratory assistance provided by Tradescan Group, Bangladesh, as well as the contributions of members of the first author's research team in Bangladesh. The support of the local government of West New Britain province of Papua New Guinea in supplying volcanic ash is also gratefully acknowledged.

References

[1] Davidson CI, Harrington JR, Stephenson MJ, Small MJ, Boscoe FP, Gandley RE. Seasonal variations in sulfate, nitrate and chloride in the Greenland ice sheet: relation to atmospheric concentrations. Atmos Environ 1989;23(11):2483–93.
[2] Seinfeld JH, Pandis SN. Atmospheric chemistry and physics – from air pollution to climate change. New York: John Wiley & Sons Inc.; 1998.
[3] Sabbioni C, Zappia G, Riontino C, Blanco-Varela MT, Aguilera J, Puertas F, et al. Atmospheric deterioration of ancient and modern hydraulic mortars. Atmos Environ 2001;35:539–48.
[4] Soroka I, Carmel D. Durability of external renderings in a marine environment – durability of building materials. Amsterdam: Elsevier Science Publishers; 1987.
[5] Leysen L, Roekens E, Van Grieken R. Air-pollution-induced chemical decay of a sandy – limestone cathedral in Belgium. Sci Total Environ 1989;78(1):263–87.
[6] Perry SH, Duffy AP. The short-term effects of mortar joints on salt movement in stone. Atmos Environ 1997;31(9):1297–305.
[7] Lee J-S, Moon H-Y. Salinity distribution of seashore concrete structures in Korea. Build Environ 2006;41(10):1447–53.
[8] Meira GR, Andrade C, Padaratz IJ, Alonso C, Borba Jr JC. Chloride penetration into concrete structures in the marine atmosphere zone – relationship between deposition of chlorides on the wet candle and chlorides accumulated into concrete. Cem Concr Comp 2007;29(9):667–76.
[9] Jaegermann C. Effect of water–cement ratio and curing on chloride penetration into concrete exposed to Mediterranean Sea climate. ACI Mater J 1990;87(4):333–9.
[10] Meira GR, Padaratz IJ, Alonso C, Andrade C. Effect of distance from the sea on chloride aggressiveness in concrete structures in Brazilian coastal site. Mater Constr 2003;53(271–272):179–88.
[11] Mustafa MA, Yusof KM. Atmospheric chloride penetration into concrete in semi-tropical marine environment. Cem Concr Res 1994;24(4):661–70.
[12] Fitzgerald JW. Marine aerosols: a review. Atmos Environ 1991;25A(93–94):533–45.
[13] McDonald RL, Unni CK, Duce RA. Estimation of atmospheric sea salt dry deposition: wind speed and particle size dependence. J Geophys Res 1982;87(C2):1246–50.
[14] Gustafsson MER, Franzén LG. Dry deposition and concentration of marine aerosols in a coastal area, Sweden. Atmos Environ 1996;30(6):977–89.
[15] Morcillo M, Chico B, Mariaca L, Otero E. Salinity in marine atmospheric corrosion: its dependence on the wind regime existing in the site. Corros Sci 2000;42(1):91–104.
[16] Petelski T, Chomka M. Sea salt emission from the coastal zone. Oceanologia 2000;42(4):399–410.
[17] Meira GR, Andrade C, Padaratz IJ, Alonso C, Borba Jr JC. Measurements and modeling of marine salt transportation and deposition in a tropical region in Brazil. Atmos Environ 2006;40(29):5596–607.
[18] Cole IS, Paterson DA, Ganther WD. Holistic model for atmospheric corrosion – part 1 – theoretical framework for production, transportation and deposition of marine salts. Corros Eng Sci Technol 2003;38(2):129–34.
[19] Cole IS, Paterson DA. Holistic model for atmospheric corrosion – part 5 – factors controlling deposition of salt aerosol on candles, plates and buildings. Corros Eng Sci Technol 2004;39(2):125–30.
[20] Hossain KMA. Deposition of marine salts and its impact on local infrastructure. Research Report no. CE-SE02-01. Lae: The Papua New Guinea University of Technology; 2001. 52p.
[21] Hossain KMA, Lachemi M. Use of volcanic debris in innovative construction and for sustainable development of volcanic areas. In: Proc. 2nd int. conference on construction in the 21st Century (CITC-II), 10–12 December, Hong Kong; 2003. p. 701–6 [Paper no. 113].
[22] Mehta PK. Concrete technology for sustainable development. Concrete Int 1999;21(11):47–53.
[23] Hossain KMA. Blended cement using volcanic ash and pumice. Cem Concr Res 2003;33(10):1601–5.
[24] Hossain KMA, Lachemi M. Development of volcanic ash concrete: strength, durability and micro-structural investigations. ACI Mater J 2006;103(1):11–7.
[25] ASTM C270. Standard specification for mortar for unit masonry. West Conshohocken (PA, USA): ASTM International; 2007.
[26] ASTM C150. Standard specification for Portland cement. West Conshohocken (PA, USA): ASTM International; 2007.
[27] ASTM C618. Standard specification for coal fly ash and raw or calcined natural pozzolan for use in concrete. West Conshohocken (PA, USA): ASTM International; 2008.
[28] ASTM C144. Standard specification for aggregate for masonry mortar. West Conshohocken (PA, USA): ASTM International; 2004.
[29] ASTM C207. Standard specification for hydrated lime for masonry purposes. West Conshohocken (PA, USA): ASTM International; 2006.
[30] ASTM C185. Standard test method for air content of hydraulic cement mortar. West Conshohocken (PA, USA): ASTM International; 2002.
[31] ASTM C1506. Standard test method for water retention of hydraulic cement-based mortars and plasters. West Conshohocken (PA, USA): ASTM International; 2003.
[32] ASTM C1437. Standard test method for flow of hydraulic cement mortar. West Conshohocken (PA, USA): ASTM International; 2007.
[33] ASTM C39/C39M. Standard test method for compressive strength of cylindrical concrete specimens. West Conshohocken (PA, USA): ASTM International; 2005.
[34] ASTM C496/C496M. Standard test method for splitting tensile strength of cylindrical concrete specimens. West Conshohocken (PA, USA): ASTM International; 2004.
[35] Tang L, Nilsson L-O. Rapid determination of chloride diffusivity in concrete by applying electrical field. ACI Mater J 1992;89(1):49–53.
[36] Hossain KMA, Lachemi M. Corrosion resistance and chloride diffusivity of volcanic ash blended cement mortar. Cement Concrete Res 2004;34(4):695–702.
[37] Lachat Instruments – QuikChem 8000. Milwaukee (WI, USA): Lachat Instruments Company; 2007. <www.lachatinstruments.com>.
[38] Orlova NV, Westall JC, Rehani M, Koretsky MD. The study of chloride ion migration in reinforced concrete under cathodic protection. Report no. FHWA-OR-RD-00-03. Sponsored by Oregon Department of Transportation and Federal Highway Administration – Washington, September 1999. 83p.
[39] ISO 10304-1. Water quality – determination of dissolved anions by liquid chromatography of ions – Part 1: determination of bromide, chloride, fluoride, nitrate, nitrite, phosphate and sulfate in waste water; 2007.
[40] Ping G, Ping X, Yan F, Beaudoin JJ. Microstructural characterization of cementitious materials: conductivity and impedance method. Materials science of concrete IV. Westerville (OH): The American Ceramic Society; 1995. p. 201–62.
[41] Montemor MF, Simoes AMP, Salta MM. Effect of fly ash on concrete reinforcement corrosion studied by EIS. Cem Concr Compos 2000;22:175–85.
[42] Hossain KMA. Chloride induced corrosion of reinforcement in volcanic ash and pumice based blended concrete. Cem Concr Compos 2005;27(3):381–90.

[43] Koulombi N, Batis G, Malami CH. In: Costa JM, Mercer AD editors., Progress in the understanding and prevention of corrosion. vol. 1, UK: The Institute of Materials; 1993. p. 619.
[44] Hossain KMA. Performance of volcanic ash and pumice-based blended cements in sulphate and sulphate-chloride environments. Adv Cem Res 2006;18(2):71–82.
[45] Clement MA, Vera G, López JF, Viquiera E, Andrade A. Test method for measuring chloride diffusion coefficients through nonsaturated concrete. Part I – the instantaneous plane source diffusion case. Cem Concr Res 2002;32(7):1113–23.
[46] Andrade C. Calculation of chloride diffusion coefficients in concrete from ionic migration measurements. Cem Concr Res 1993;23(3):724–42.